Proceedings of the ASME 2022 17th International Manufacturing Science and Engineering Conference
MSEC2022
June 27-July 1, 2022, Virtual, Online

MSEC2022-85680

SIZE-BASED FILTRATION OF POLY-DISPERSE MICRO-PARTICLE BY DIPPING

Md Ibrahim Khalil
Mechanical Engineering Department University of Maine, Orono
Maine, ME

Bashir Khoda, Ph.D.*
Mechanical Engineering Department
University of Maine, Orono
Maine, ME

ABSTRACT

In manufacturing industries, spherical micro- particles are commonly used as (e.g., brazing powder, metal filler, and 3D printing powder) which are produced with droplet-based particle fabrication techniques. Such processes create spherical morphology but introduce polydispersity and follow a continuous exponential pattern commonly expressed with Rosin-Rammler expression. Sorting those micro-particles in a narrower size range is an important but difficult, costly, and challenging process. Here we demonstrate the successful separation of the particles from a poly-disperse mixture with a particle volume fraction of 10% by dipping process. Nickel-based micro-particles (avg. dia. 5.69 μm) are added in a binder-based liquid carrier system. To encounter the gravitational force, external kinetic energy in the form of agitation is applied to ensure the uniform dispersion of the particles. The cylindrical substrate is prepared and dipped in the 'pseudo suspension' to separate the particles by adhering to it. The substrate is dried, and images are taken to characterize the separated particles using image J software. A clear size distribution can be observed which is also plotted. Additionally, a relationship between the process parameter and sorted particles has been established. The proposed method is quick, controllable, and easy to implement, which can be a useful tool for sorting wide-range poly-disperse particles.

Keywords: sorting, poly-disperse particle, micro-particle, entrapment factor.

NOMENCLATURE

ϕ_p	volume fraction of particles
V_p	volume of particles
V_{solute}	volume of binder
$V_{solvent}$	volume of solvent
$\dot{\gamma}$	shear rate
η_ϕ	viscosity of suspension
η_0	viscosity of solution
ϕ_{max}	maximum volume fraction of particles
$[\eta]$	Intrinsic viscosity

1. INTRODUCTION

Granular materials or powder particles are the smaller unit volume of material, composite, or alloy with various sizes, shapes, and morphology. Both organic and inorganic materials are commonly found in particle form and their demand is increasing rapidly in part production for specialized applications including medical devices, implants, tools, mold, paint, and coating technology [1-3]. Powder metallurgy, sintering process [4], Metal injection molding (MIM), powder forging, Powder Based Fusion (PBF) [5], electron beam melting (EBM), etc. are common powder-based manufacturing processes. Some common powder manufacturing processes are plasma rotating electrodes, plasma atomization, and gas atomization. Some researchers classified the particles as single crystals, polycrystals, or glass [3] while others classified the particles as metals, polymers, and composites [6]. However, the particles manufactured by using these processes are mostly poly-disperse particles as the standard deviation of the size of the particles is often large. Rosin-rammler exponential expression is commonly used to express their size distribution function [7]. Polydispersity in particles is very common and may create challenges in the fabricated part. For example, homogeneity in the melt pool is affected due to the polydispersity in the powder bed fusion process [5]. Thus, uniformity in particle size or mono-dispersity is desirable in industrial applications such as additive manufacturing [8-11], powder sintering, metal injection molding, powder bed fusion, etc. [12].

Manufacturing of the mono-disperse particle is very costly and challenging [13], filtration of bulk particles is often performed as a post-processing activity to achieve a narrow particle size range. Some of the common particle filtration processes are centrifugation [14], membrane filtration [15], and the motion of bubbles [16]. However, current filtration processes bring challenges such as clogging during the particle filtration process. We reported the entrapment phenomenon (forces related to entrapment) of the particles and subsequent filtration in one of our previous works [17]. This work is focused on the rheology of suspension with respect to the entrapped particle. An empirical relationship between the particle size and viscosity

variation has been developed that can be used to determine the characteristics of the mixture and filtered particle sizes. When a substrate is dipped into a polymer solution a thin polymer layer is formed over the substrate. When particles get in contact with the polymer layer, they can entrap particles in submerged conditions. Here, we investigate this phenomenon considering various parameters such as relative speed, fluid viscosity, particle loading, etc. Our result shows that the size of the entrapped particles can be controlled by controlling the process parameter.

2. METHODOLOGY

In order to study the filtration of poly-disperse particles, cylindrical metal substrate of AISI 1006 mild steel rod and the average diameter of the substrate is 1.1 mm (procured from ClampTite LLC) is used. Rod samples are cleaned in an ultrasonic bath with acetone at 50°C for 10 minutes to remove any surface contaminants and passive films. The dipping suspension is prepared using solvent (1, 3-Dioxolane), solute (binder), and solid brazing (Nicrobraz 51) particles. The solvent (1, 3 dioxolane) used in this experiment has good solubility for the binder (PMMA) and the binder is completely dissolved after two hours of stirring at room temperature. The dissolution crates good solution and no gel formation is found by Dynamic Light Scattering (DLS) experiment which is done by Zetasizer equipment. Moreover, the transparent solution helps better control over the dipping experiment, that is why this pair of solute and solvent are used in the experiments. The solute and solvent are called the liquid carrier system (LCS) for the experiments. Brazing powder (Nicrobraz 51; Wall Colmonoy company, Ohio; Spherical dia range ~0-100 µm) is sieved with Gilson Performer III shaker through Stainless Steel 635 Mesh (20 µm) in our lab to reduce polydispersity. SEM image is taken for the supplier provided Nicrobraz particle (avg dia = 44 µm). To reduce the polydispersity, we use 20 µm sieve and the average diameter becomes 5.69 µm. The volume fraction of the particles is calculated by taking the ratio of particles' volume and the total volume of the mixture (solute, solvent, and particles) as

$$\phi_p = V_p/(V_p + V_{solute} + V_{solvent}) \quad (1)$$

here V_p is the volume of particles. The binder concentration is varied at different intervals ranging from 1% to 13% for the sorting of the particles within the range of particles used in the mixture. On the other hand, the volume fraction of the particles is kept constant (ϕ_p= 10%) for our experiments as the previous studies have found that the mixture with $\phi_p < 20\%$ remains in the Newtonian regime at a low share rate, $\dot{\gamma}$ [18]. Poly-methyl methacrylate (PMMA) is used as the binder, and the chemical formula of the binder is CH_2=C[CH_3]CO_2H (Sigma Aldrich, USA). To dissolve the solute into the solvent, a magnetic stirrer is used at room temperature for two hours.

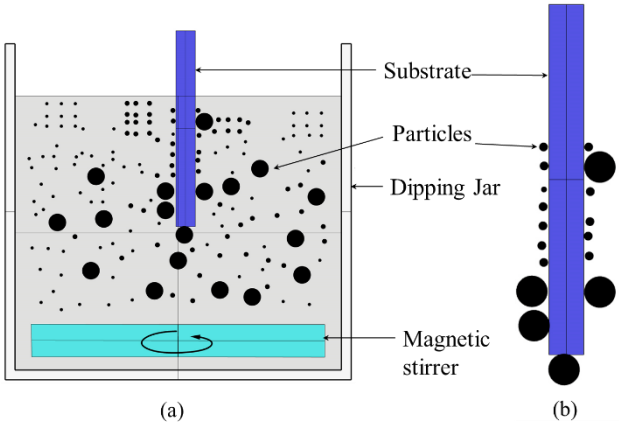

FIGURE 1: SCHEMATIC OF THE EXPERIMENTAL SETUP (a) ROD AFTER WITHDRAWAL FROM SUSPENSION (b)

The density of both the binder and the solvent are 1.17 g/cm^3 and 1.06 g/cm^3 respectively at room temperature (RT = 25°C). On the other hand, the density of the particles is 7.8 g/cm^3, and the particle to liquid density ratio is >7. Due to the high-density ratio of the solution and the particles, a magnetic stirrer is used to keep the particles suspended during the experiments. The dipping jar used in this experiment is a 20 mL 95020-0CV Vials, screw top; clear borosilicate glass, and round bottom with the dimension of 75.5 x 22.5mm. The schematic of the experimental setup is shown in figure 1. During the experiment, the rod is inserted at the center at a speed of 10 mm/s. The stirrer is kept on for the first fifty minutes before being turned off and the dipping rod remains submerged for 40 minutes as the mixture settled down, resulting in a phase-separated mixture. The entire duration of the experiment is 90 minutes. This guarantees that no particles float in the mixture and entrain the substrate during the withdrawal process. Afterward, the substrate is withdrawn from the suspension very slowly (0.1 mm/s) to avoid the effect of the vibration. Once extracted, the substrate is put under the microscope, and images are taken for analysis by imageJ software.

3. RESULTS AND DISCUSSION

The thickness of the polymer layer formed over the substrate is dependent on the dominance of the capillary and viscous force at the gas/liquid interface during the dip-coating process [19-21]. On the other hand, the particle entrapment process helps the particles to trap inside the thin polymer layer in submerged conditions at the solid-liquid interface. The thickness of the polymer layer over the substrate is dependent on the viscosity of the suspension which is dependent on the binder and particle volume fraction of the suspension. The variation of the different components of the suspension during the experiments is listed in table 1.

The viscosity of the solution is measured using the Anton Paar MCR 302 Rheometer with a 50 mm parallel plate/plate geometry at a variable shear rate (1-1000 S^{-1}). The flow curve is shown in Figure 2. The averaged value of the viscosity of the solution at different shear is used to calculate the viscosity of the

suspension by using the Krieger-Dougherty equation [22] using the viscosity of the solution

$$\eta_\phi = \eta_0 \left(1 - \frac{\phi}{\phi_{max}}\right)^{-[\eta]\phi_{max}} \quad (2)$$

here ϕ_{max} is the maximum volume fraction of the particles and $[\eta]$ is the intrinsic viscosity. For the rigid sphere under sheared suspensions, the maximum particle volume fraction is reported ϕ_{max} = 0.67 [23] and $[\eta] = 2.5$ [24] to calculate the viscosity of the suspension.

TABLE 1: VARIATION OF THE COMPONENTS OF SUSPENSION

Binder volume fraction (%)	Particle volume fraction (%)	Solvent volume fraction (%)
1	10	89
2	10	88
4	10	86
7	10	83
10	10	80
13	10	77

After the withdrawal of the substrate from the suspension and drying very carefully, the imaging of the substrate is done using VHX 7000 Digital 4K microscope (KEYENCE corp., IL). The high-resolution 4K images of the dipped rod are analyzed with imageJ software. The images of the sorted particles at different viscosities are shown in figure 3. To ensure statistical significance, ten samples (regions) are randomly selected for each measurement. The variation of the maximum and average particle size is shown in figure 4. As we observed in this regime of viscosity, the size of the entrapped particles increases exponentially with the increase in the viscosity, which is shown in the fitted curve. However, we assume the power of the exponent may reduce as the viscosity increases which can be our future work. The R-square value for both the average particle diameter and maximum particle diameter in the fitting curve is 99.64% and 99.44% respectively.

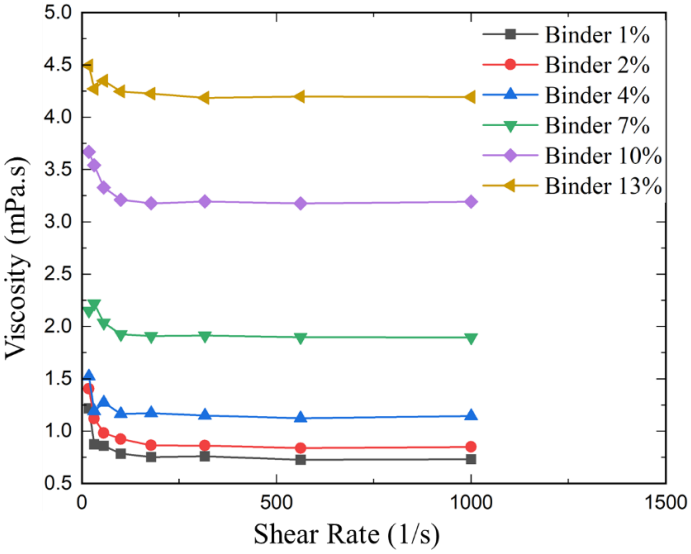

FIGURE 2: VARIATION OF THE VISCOSITY WITH SHEAR RATE

The equation of the fitted curve to find the average and maximum particle diameter is $A_1 * exp\ exp\left(\frac{x}{t_1}\right) + y_0$ and the value of the constants is y_0= -5.99±3.037, A_1= 6.29±2.72 and t_1= 10^{-4}±0.001 for the average particle size.

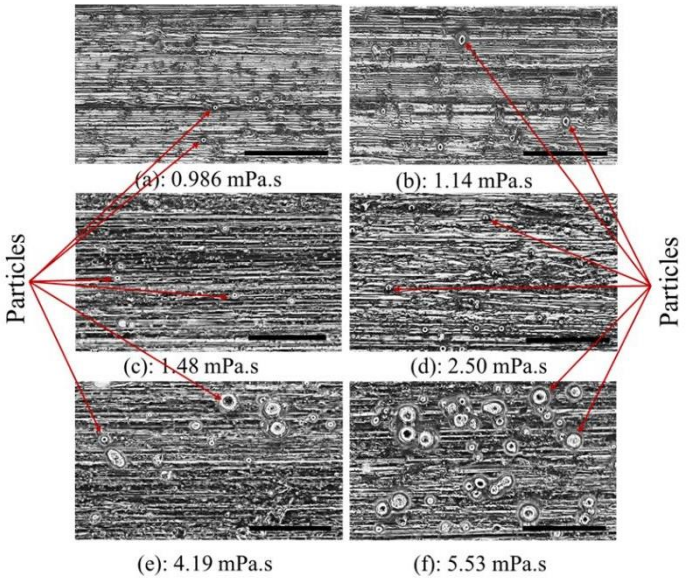

FIGURE 3: EXPERIMENTAL IMAGES OF THE FILTERED PARTICLES AT DIFFERENT VISCOSITIES

On the other hand, the value of the constants for the maximum particle diameter is y_0= -0.93±0.98, A_1= 1.73±0.86 and t_1= 10^{-4}±0.001. The above-mentioned equation can be used to predict the entrapped particle size at different viscosity of the suspension. Moreover, the viscosity of the suspension can be optimized for filtration to obtain the desired particle size.

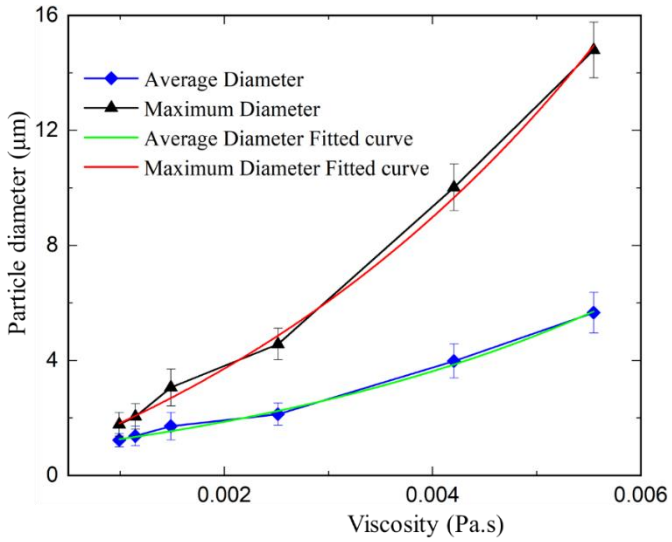

FIGURE 4: VARIATION OF PARTICLE SIZE WITH THE VARIATION OF VISCOSITY

To measure the effectiveness of the filtration process, the sorted particles are counted, and diameter is measured for their distribution. Figure 5 represents the sorted particle distribution after dipping at different viscosity ranges. The first portion of figure 5 shows the distribution of particles before filtration (the distribution of bulk particles). On the other hand, the next three regions of the TA show the distribution of the particles found at different viscosity ranges of the suspension. For better visualization, the Weibull distribution is fitted over the histogram. The narrow zone of particle diameter in the low viscous suspensions indicates the smaller particle size is entrapped on the substrate and this range of Weibull distribution with the increase of the viscosity. This clearly shows the particle filtration process. Clogging is common in traditional (centrifugation and membrane) filtration processes. The life of the mesh is reduced significantly with polydisperse particles, and the time required for filtration is exponential increases. This study used the capillary action for the filtration process which is free from clogging and a relatively fast process.

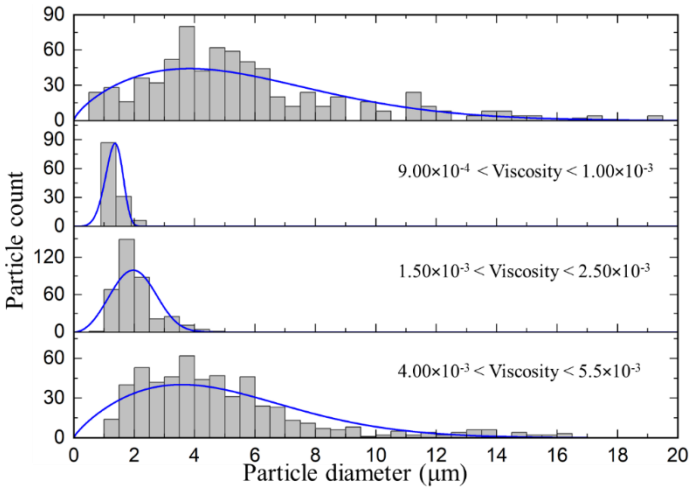

FIGURE 5: DISTRIBUTION OF PARTICLES AT DIFFERENT VISCOSITY RANGES

The exponential fit is adopted here, and the statistical R^2 values indicate that the fitted equations are very close to the experimental values. These equations can be used to predict the size of the particles at the time of filtration. This process successfully shows the filtration of the particles from density-mismatching suspensions using entrapment. The added energy provided by the stirring of the mixture helps the creating a pseudo suspension. The particles in the mixture observe kinetic energy which increases their probability to collide with the substrate and hence the entrapment occurs. Most organic particles have a lower density that produces a density matching solution with LCS. We anticipate similar entrapment phenomena may occur and sorting phenomena may be observed. However, we have not performed any experiments with organic particles.

4. CONCLUSION

Polydispersity in particle distribution can cause challenges in the powder-based manufacturing process. Achieving narrow particle size distribution in the sub-micron range is time-consuming, costly, and resource intensive. This work successfully presents the size-based particle filtration of the poly-disperse particle mixture from the density mismatching suspension using entrapment in submerged conditions. The process is simple, easy, quick, and can be scaled up by increasing the number of substrates or by adding dipping jars in series. In this works the density of the particles used is almost eight times higher than the solution. For our experiment, the volume fraction of the particles is kept fixed (10%) and the size of the entrapped particles over the substrate is observed to visualize the filtration effect. Moreover, the distribution of the particles confirms the filtration effect. By continuing the repetition of the experiment, this process can filter a narrow range of particle sizes on large scale.

ACKNOWLEDGEMENTS

The authors thank Alex Watson and John Belding, Director of Advanced Manufacturing Center (AMC) for helping with the

microscopy. Financial supports from Grant NSF-CMMI # 2101751, US-DOT # 693JK31850009CAAP and UMaine-NEU Seed Grant are acknowledged.

REFERENCES

[1] R. van Noort, "The future of dental devices is digital," (in eng), *Dent Mater,* vol. 28, no. 1, pp. 3-12, Jan 2012.

[2] B. Lestarquit, "Geometry of a paint film: Basics revisited," *Progress in Organic Coatings,* vol. 90, pp. 200-221, 2016/01/01/ 2016.

[3] J. Evans and L. De Jonghe, *The Production and Processing of Inorganic Materials*. Springer, 2016.

[4] W. Licht, "Particle size measurement: Second edition, T. Allen, Chapman and Hall, London (1975). 454 pages. $25.95," *Aiche Journal,* vol. 22, pp. 202-202, 1976.

[5] J. Volpp, "Powder particle movement during Powder Bed Fusion," *Procedia Manufacturing,* vol. 36, pp. 26-32, 2019/01/01/ 2019.

[6] A. Noskov, T. K. Ervik, I. Tsivilskiy, A. Gilmutdinov, and Y. Thomassen, "Characterization of ultrafine particles emitted during laser-based additive manufacturing of metal parts," *Scientific Reports,* vol. 10, no. 1, p. 20989, 2020/12/02 2020.

[7] M. Alderliesten, "Mean Particle Diameters. Part VII. The Rosin-Rammler Size Distribution: Physical and Mathematical Properties and Relationships to Moment-Ratio Defined Mean Particle Diameters," *Particle & Particle Systems Characterization,* https://doi.org/10.1002/ppsc.201200021 vol. 30, no. 3, pp. 244-257, 2013/03/01 2013.

[8] Y. Bai, C. Wall, H. Pham, A. Esker, and C. B. Williams, "Characterizing Binder–Powder Interaction in Binder Jetting Additive Manufacturing Via Sessile Drop Goniometry," *Journal of Manufacturing Science and Engineering,* vol. 141, no. 1, 2018.

[9] C. Y. Park and T. I. Zohdi, "Numerical Modeling of Thermo-Mechanically Induced Stress in Substrates for Droplet-Based Additive Manufacturing Processes," *Journal of Manufacturing Science and Engineering,* vol. 141, no. 6, 2019.

[10] B. Khoda, A. M. M. N. Ahsan, A. N. Shovon, and A. I. Alam, "3D metal lattice structure manufacturing with continuous rods," *Scientific Reports,* vol. 11, no. 1, p. 434, 2021/01/11 2021.

[11] B. Khoda and A. M. M. N. Ahsan, "A Novel Rapid Manufacturing Process for Metal Lattice Structure," *3D Printing and Additive Manufacturing,* 2021.

[12] A. Rota, T. V. Duong, and T. Hartwig, "Micro powder metallurgy for the replicative production of metallic microstructures," *Microsystem Technologies,* vol. 8, no. 4, pp. 323-325, 2002/08/01 2002.

[13] E. W. Sequeiros, O. Emadinia, M. T. Vieira, and M. F. Vieira, "Development of Metal Powder Hot Embossing: A New Method for Micromanufacturing," *Metals,* vol. 10, no. 3, 2020.

[14] J. C. Giddings, "Field-flow fractionation: analysis of macromolecular, colloidal, and particulate materials," (in eng), *Science,* vol. 260, no. 5113, pp. 1456-65, Jun 4 1993.

[15] R. Baker, "Membrane technology in the chemical industry: future directions," *Membrane technology in the chemical industry,* 2001.

[16] Y. E. Yu, S. Khodaparast, and H. A. Stone, "Separation of particles by size from a suspension using the motion of a confined bubble," *Applied Physics Letters,* vol. 112, no. 18, pp. 181604-181604, 2018.

[17] I. Khalil and B. Khoda, "Sorting of Poly-Disperse Particle by Entrapment Using Liquid Carrier System," *Journal of Manufacturing Science and Engineering,* vol. 144, no. 5, 2021.

[18] S. Dhar, S. Chattopadhyay, and S. Majumdar, "Signature of jamming under steady shear in dense particulate suspensions," *Journal of Physics: Condensed Matter,* vol. 32, no. 12, p. 124002, 2019/12/19 2019.

[19] B. Khoda, A. M. M. Nazmul Ahsan, and S. M. N. Shovon, "Solid Transfer of Large Particles by Dipping in a Heterogeneous Mixture," presented at the ASME 2021 16th International Manufacturing Science and Engineering Conference, 2021. Available: https://doi.org/10.1115/MSEC2021-64079

[20] A. Sauret, A. Gans, B. Colnet, G. Saingier, M. Z. Bazant, and E. Dressaire, "Capillary filtering of particles during dip coating," *Physical Review Fluids,* vol. 4, no. 5, 2019.

[21] B. Khoda, A. M. M. N. Ahsan, and S. M. N. Shovon, "Dip Coating From Density Mismatching Mixture," *Journal of Micro and Nano-Manufacturing,* vol. 9, no. 2, 2021.

[22] I. M. Krieger and T. J. Dougherty, "A Mechanism for Non-Newtonian Flow in Suspensions of Rigid Spheres," *Transactions of the Society of Rheology,* vol. 3, no. 1, pp. 137-152, 1959/03/01 1959.

[23] T. Kitano, T. Kataoka, and T. Shirota, "An empirical equation of the relative viscosity of polymer melts filled with various inorganic fillers," *Rheologica Acta,* vol. 20, no. 2, pp. 207-209, 1981.

[24] A. Einstein, "Berichtigung zu meiner Arbeit: „Eine neue Bestimmung der Moleküldimensionen”," *Annalen der Physik,* vol. 339, no. 3, pp. 591-592, 1911.